LA-UR-15-27786
Approved for public release; distribution is unlimited.

Title: Facility target insert shielding assessment

Author(s): Mocko, Michal

Intended for: Report

Issued: 2015-10-06

Facility target insert shielding assessment

M. Mocko, October 2015

Introduction

Main objective of this report is to assess the basic shielding requirements for the vertical target insert and retrieval port. We used the baseline design for the vertical target insert in our calculations. The insert sits in the 12”-diameter cylindrical shaft extending from the service alley in the top floor of the facility all the way down to the target location. The target retrieval mechanism is a long rod with the target assembly attached and running the entire length of the vertical shaft. The insert also houses the helium cooling supply and return lines each with 2” diameter. In the present study we focused on calculating the neutron and photon dose rate fields on top of the target insert/retrieval mechanism in the service alley. Additionally, we studied a few prototypical configurations of the shielding layers in the vertical insert as well as on the top.

Calculation approach and geometry

All the presented calculations were done using the MCNPX Monte Carlo neutron transport code (version 2.7.0). In the present calculations we updated the production facility geometry including the details of the vertical insert/retrieval mechanism. Figure 1 displays the cross-sectional view of the geometry at the beam height. We clearly recognize the two electron accelerators that deliver electron beams at 42 MeV on the Mo-100 target. The target is modeled as a solid Mo-100 cylinder with radius of 1.66 cm and 2.5 cm in length with density of 10.0 g/cm^3. In all of the presented calculations we assumed the beam current of 5.664 mA combined (for both accelerators). All the calculations listed in this report utilized ICRP 74 dose conversion coefficients for neutrons and photons.

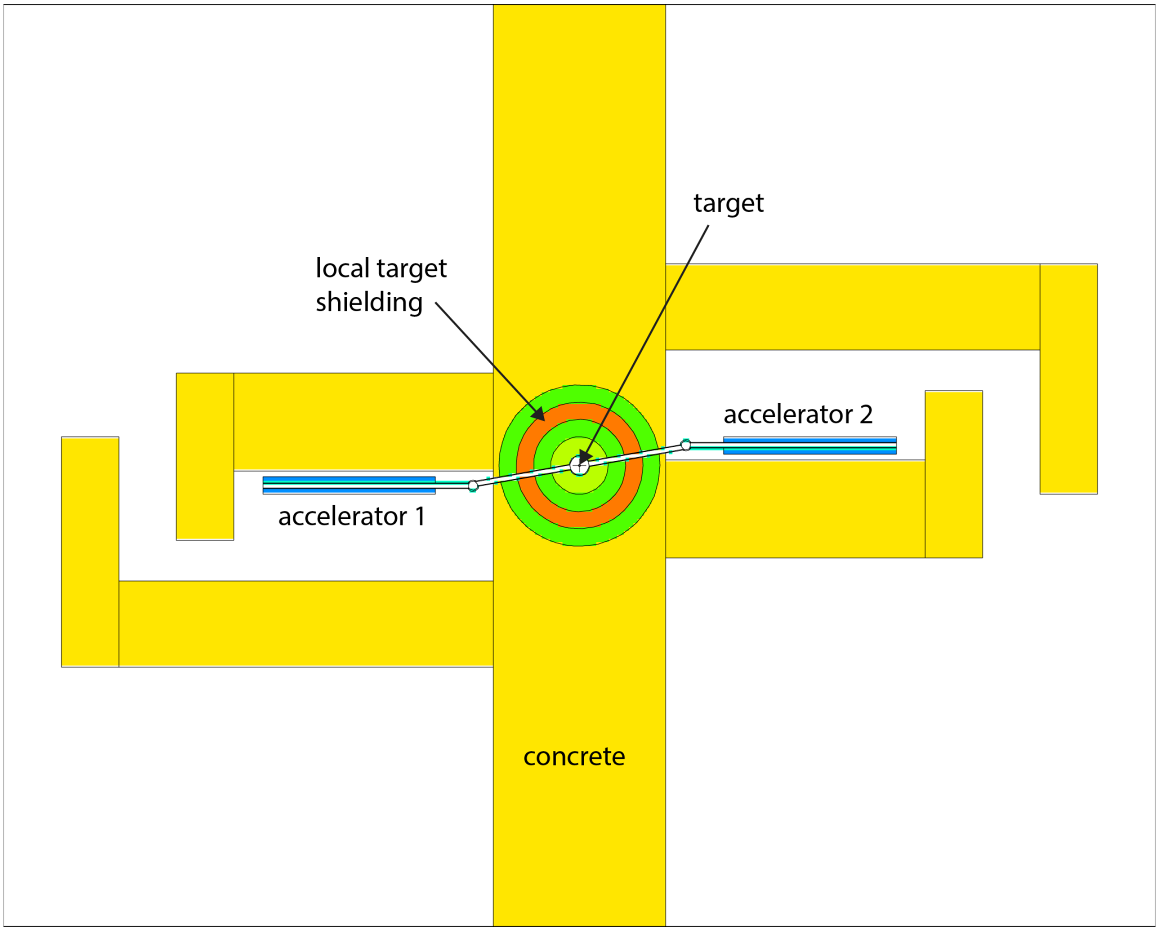

Figure 1: Cross-sectional view through the facility geometry at the electron beam height. Main components are clearly labeled for reference.

Figure 2 shows the elevation view cut through the geometry displaying the implementation of the vertical insert/retrieval mechanism in detail. The two helium-cooling lines are located in plane perpendicular to the axis of the electron beams. These lines are modeled as 2" cylindrical openings in our shielding study (void). The vertical distance between floor of the service alley and the electron beams is 362.4 cm in our geometry. This distance is filled with 304.8 cm of regular concrete (distance between the ceiling of the accelerator enclosure below and floor of the service alley above). In our geometry we also included a shielding enclosure (cylindrical) on top surrounding the access to the target insert/retrieval rod.

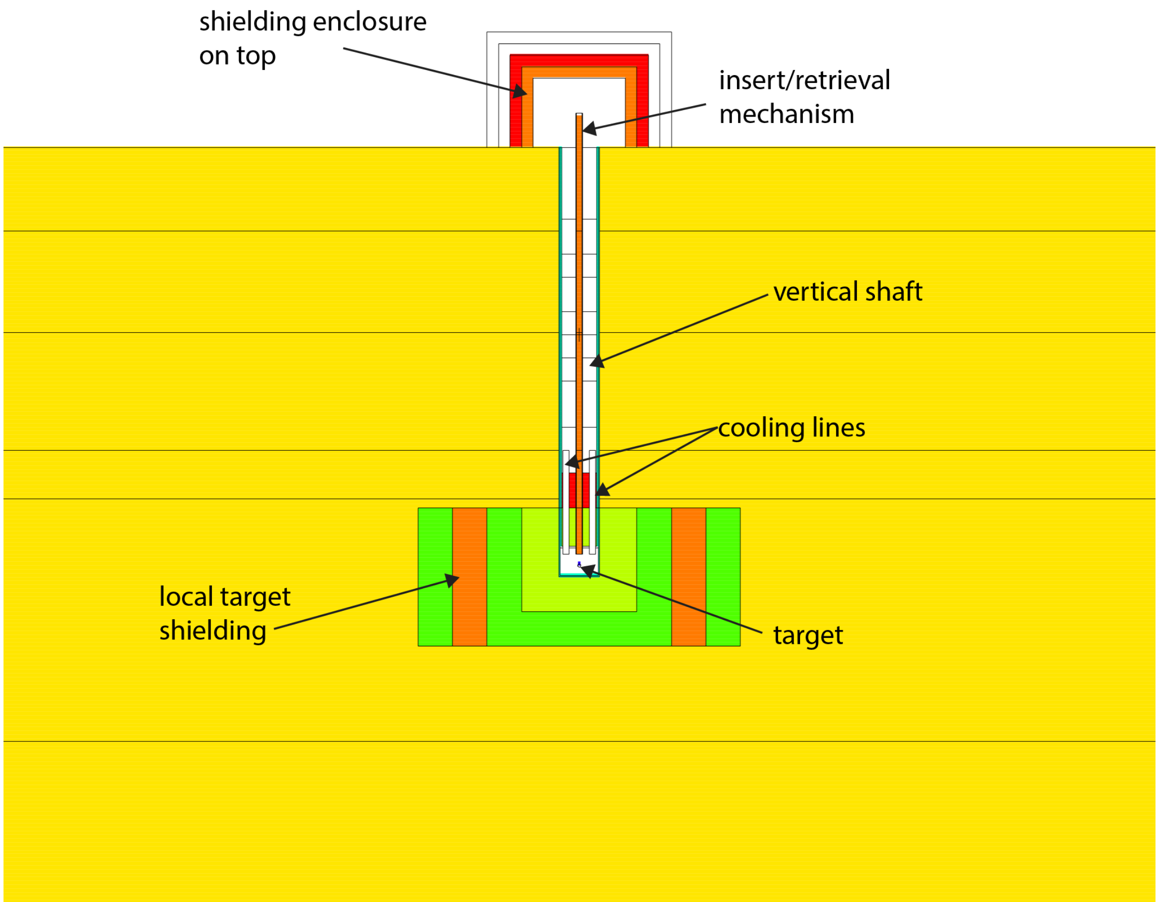

Figure 2: Elevation view of the MCNPX geometry showing the vertical target insert/retrieval mechanism. Main components of the insert as well as points of reference are clearly labeled.

The MCNPX calculations offer a fairly limited dynamic range dictated by the maximum number of histories (2.1 billion) as well as the by the cpu time limitations. To enable simulation of dose rate fields located on top (service alley) we generated secondary photon and neutron source cards on a cylindrical surface encompassing the target rod. We conveniently neglected the strongly anisotropic neutron and photon fields extending along the electron beam directions, as these will not constitute sizeable contributions to the dose fields in the vertical direction (perpendicular to the electron beam axis). The neutron and photon secondary source cards were benchmarked against the results obtained when the calculation was run with the electron beams. The geometry utilized in our benchmark exercise is shown in Figure 2. The setup includes two plugs in the bottom of the vertical insert: lead (33 cm) followed by 30% borated polyethylene (30 cm). We compared the neutron and photon dose rate fields at multiple locations at different elevations. The results are summarized in Table 1.

Table 1: Benchmark comparison of the neutron and photon secondary source. The reference calculation was run with electron beams impinging on the target. The results labeled as "SECONDARY" were obtained using the secondary neutron and photon sources starting from the cylindrical surface encompassing the target rod. For vertical distance of 300 and 400 cm we setup two tallies at different locations within the vertical insert opening, they are denoted as (+) and (-).

Tally location (vertical distance)	Neutron dose rate (mrem/h) REFERENCE	Photon dose rate (mrem/h) REFERENCE	Neutron dose rate (mrem/h) SECONDARY	Photon dose rate (mrem/h) SECONDARY
50 cm	2.36E+09	4.08E+07	2.12E+09	4.39E+07
100 cm	1.70E+07	4.03E+06	1.72E+07	4.16E+06
200 cm	2.20E+06	5.42E+05	2.32E+06	5.91E+05
300 cm (+)	7.86E+05	2.04E+05	8.67E+05	2.23E+05
300 cm (-)	7.76E+05	2.09E+05	8.40E+05	2.19E+05
400 cm (+)	4.63E+05	1.21E+05	4.96E+05	1.33E+05
400 cm (-)	4.65E+05	1.23E+05	4.82E+05	1.25E+05

In our calculations we tallied neutron and photon dose rate fields in both, the calculation run with a neutron as well as a photon source. Results listed in Table 1 include the sum of the contributions generated by photons and neutrons. It is worthwhile noting that overwhelming majority (80-90%) of neutron dose comes from the calculation run with a neutron source (same applies for photons).

From the results of our benchmarking study we conclude that our neutron and photon source cards are setup appropriately and they are reproducing the dose rate fields at different vertical distances in the vertical target insert/retrieval shaft.

After this benchmarking exercise we can use neutron and photon source cards for subsequent studies of the different shielding options for the vertical target insert mechanism.

Results and discussion

When evaluating the dose rates on top of the vertical target insert/retrieval mechanism we utilized point ring detectors placed about 20 cm above the floor of the service alley (380 cm over the electron beam axis). The dose rates were calculated using ICRP-74 dose conversion factors as stated above.

The first geometry in our study included a setup with minimal amount of shielding material. The geometry is displayed in Figure 2 we note there are two plugs of lead followed by borated polyethylene (30 cm and 30 cm). This geometry was utilized in our benchmarking exercise. We note that the dose rates in the service alley are approximately 500 rem/hr neutron and 150 rem/hr photon. These are substantial radiation fields albeit we need to keep in mind that they are strongly focused in the vertical direction (see Figure 6). One could envision designing a shielding enclosure restricting personnel access near the helium cooling lines (and target retrieval mechanism) providing attenuation of the streaming radiation in the vertical direction. The radiation fields are falling rather fast as a function of radius (from the axis of the target retrieval mechanism). This approach would leave the area on top of the shielding enclosure (and on building roof) as radiation areas with personnel access prohibited during beam operations. A detailed analysis of skyshine effects will be required for this option.

There are two major streaming paths for radiation (neutron and photon) to reach the service alley, they are the supply and return pipes for helium cooling (2" diameter each). To reduce the dose rate fields on top of the vertical target insert we studied different number of doglegs in the cooling lines along with introduction of more shielding material in the vertical shaft.

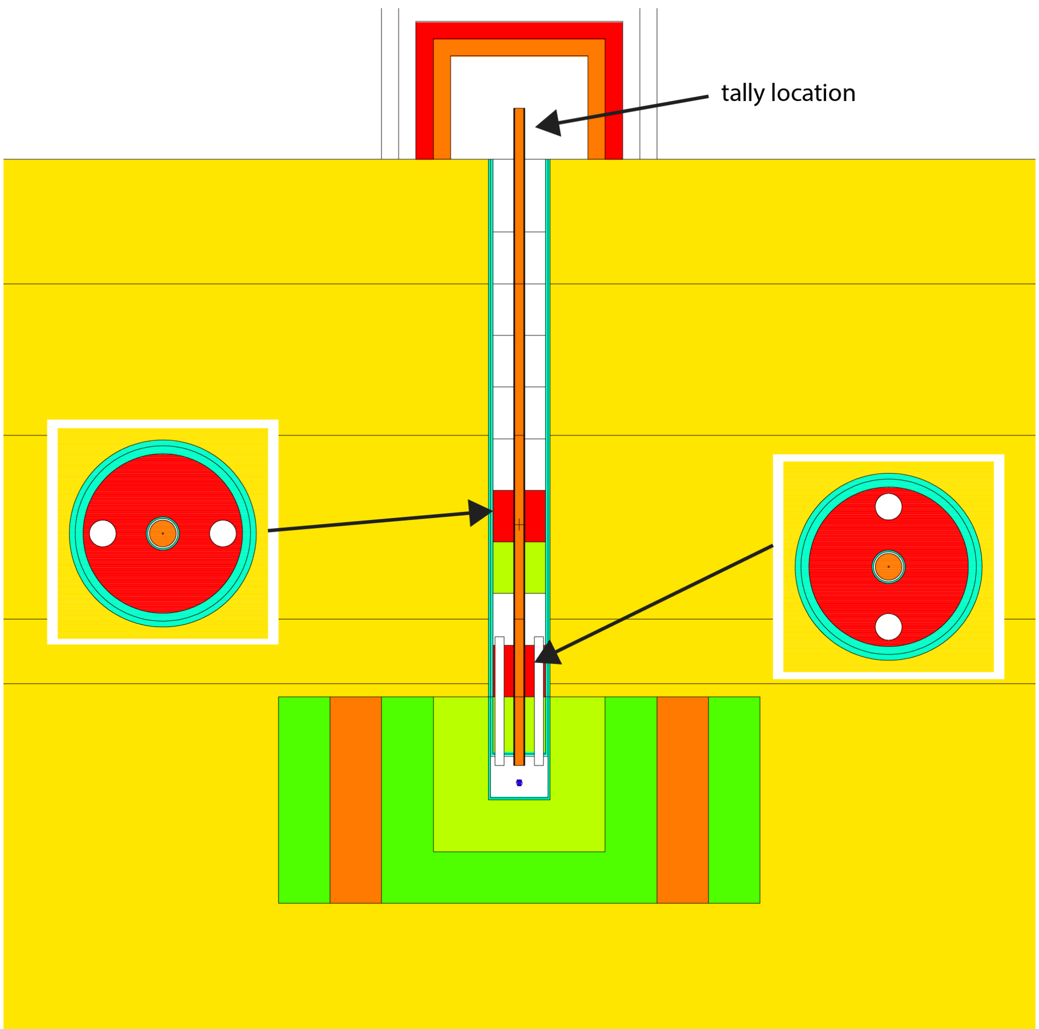

Figure 3: MCNPX geometry with one dogleg in the helium cooling lines.

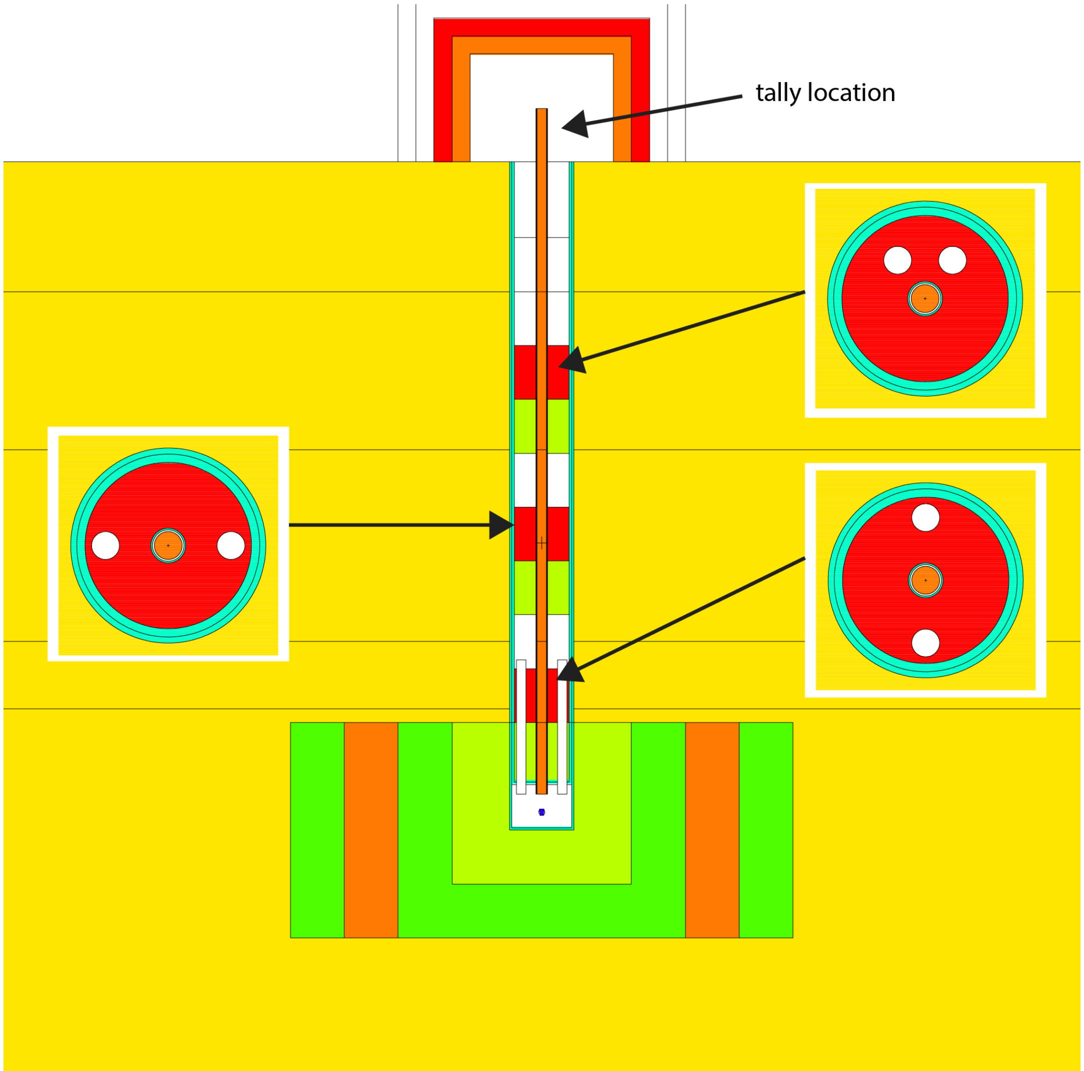

Figure 4: MCNPX geomety with two doglegs in the helium cooling lines.

To minimize the streaming radiation through the helium cooling lines we introduced doglegs. In Figure 5 we notice that after the first dogleg the cooling lines plane is rotated 90 degrees with respect to the first leg. In the next we put both cooling lines in the top half and in the last leg they are located in the lower half of the cross section view. Due to the nature of these calculations we did not implement the doglegs in our geometry, but rather left 30-cm tall void gaps in the shielding stack building conservatism in our calculations.

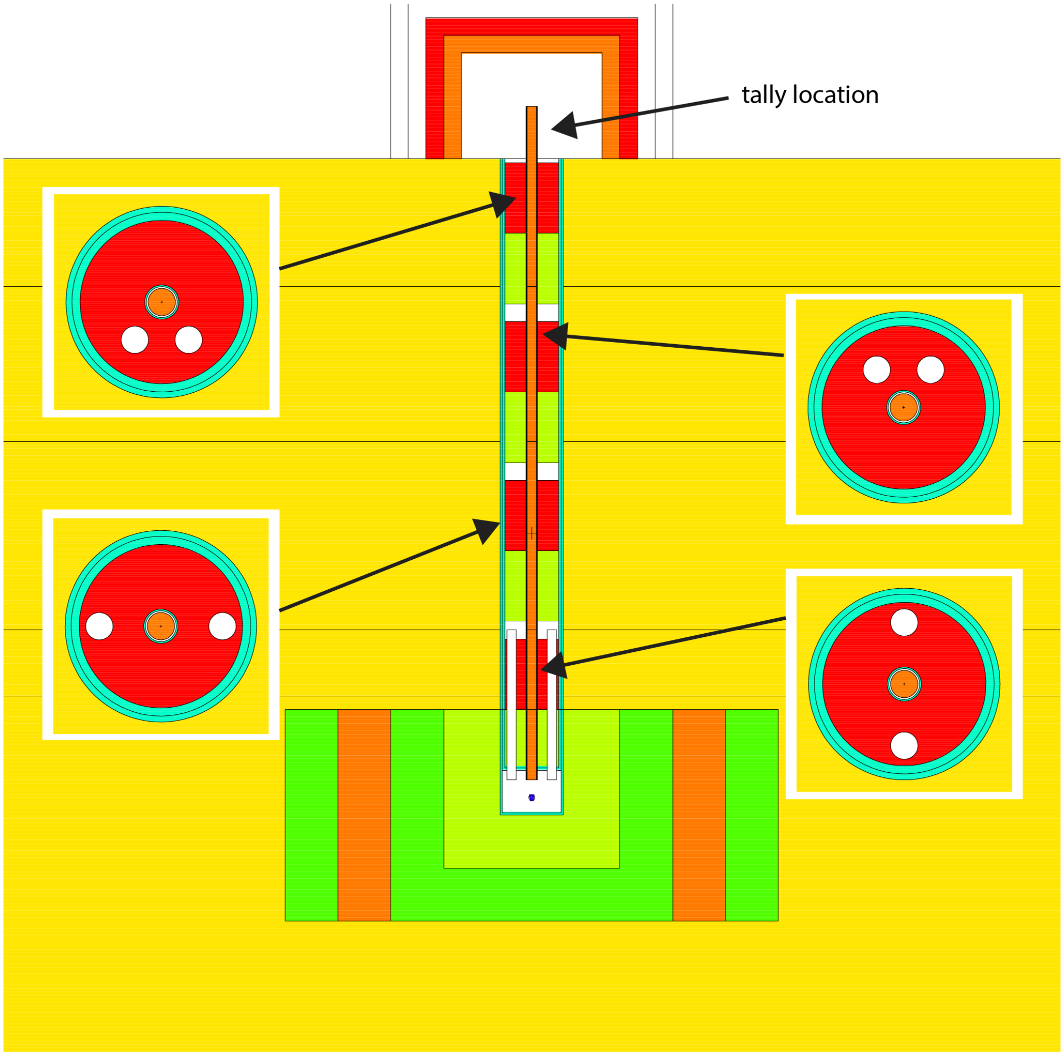

Figure 5: MCNPX geometry with three doglegs in the helium cooling lines.

The configurations of doglegs in the helium lines are shown in Figures 3-5. With increasing number of doglegs in the helium cooling lines we are also increasing the amount of shielding material in the vertical shaft. Every dogleg is followed by a steel and borated polyethylene plug of 30 cm tall each. In Table 2 we list the highest recorded neutron and photon dose rates on top (tally location is depicted in each geometry figure). The dose rates have been tallied with multiple point detectors on top and we are reporting the highest recoded dose rate numbers in Table 2.
We notice that introducing one dogleg in the helium cooling lines results in drastic (two orders of magnitude) drop in dose rates for both neutrons and photons. However, further addition of doglegs and additional shielding plugs does not lower the dose rate consequences tangibly. This behavior clearly indicates that these dose rates are dominated by a different process (streaming path) not influenced by our geometry changes as shown in Figures 3-5.

Table 2: Neutron and photon dose rates calculated for different configurations of the helium cooling lines bends. See text for details

configuration	Neutron dose rate on top (rem/hr)	Photon dose rate on top (rem/hr)
No bends (reference)	500	150
One bend	1.8	2.2
Two bends	1.7	2.0
Three bends	1.3	1.9

A quick inspection of a run with mesh tally visualizing the dose rate fields in the geometry displays the culprit. The results are depicted in Figure 6 for neutrons and photons in left and right panels, respectively. We note a strong streaming path along the central rod acting as the target retrieval mechanism. Upon closer examination we noticed that we included a 3 mm gap between the steel rod and the surrounding pipe. See Figure 7 for close up view of the bottom end of the target insertion/retrieval mechanism. The gap was introduced in our geometry "by hand" and as such does not represent any engineering constraints or particular design. To test our hypothesis of this tiny gap causing approximately 1-2 rem/hr radiation fields on top we prepared a new geometry that does not include a gap (shown in right panel of Figure 7).

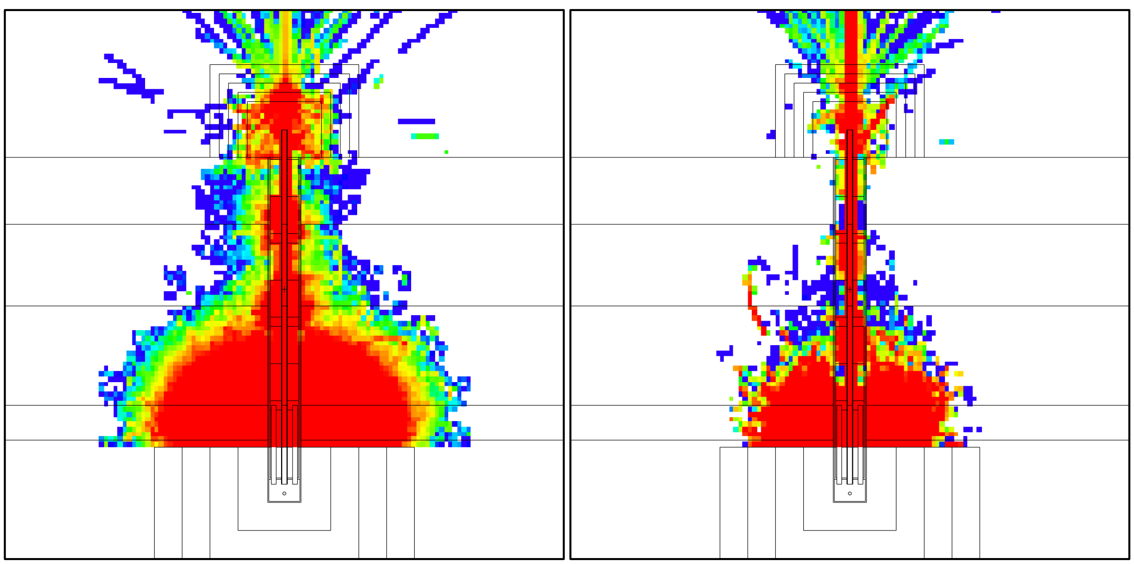

Figure 6: Mesh tally results for geometry depicted in Figure 5 visualizing the dose rate fields for neutron (left) and photons (right). Red color depicts dose rates of 1 rem/hr and higher and blue shows dose rate fields of 1 mrem/hr or lower.

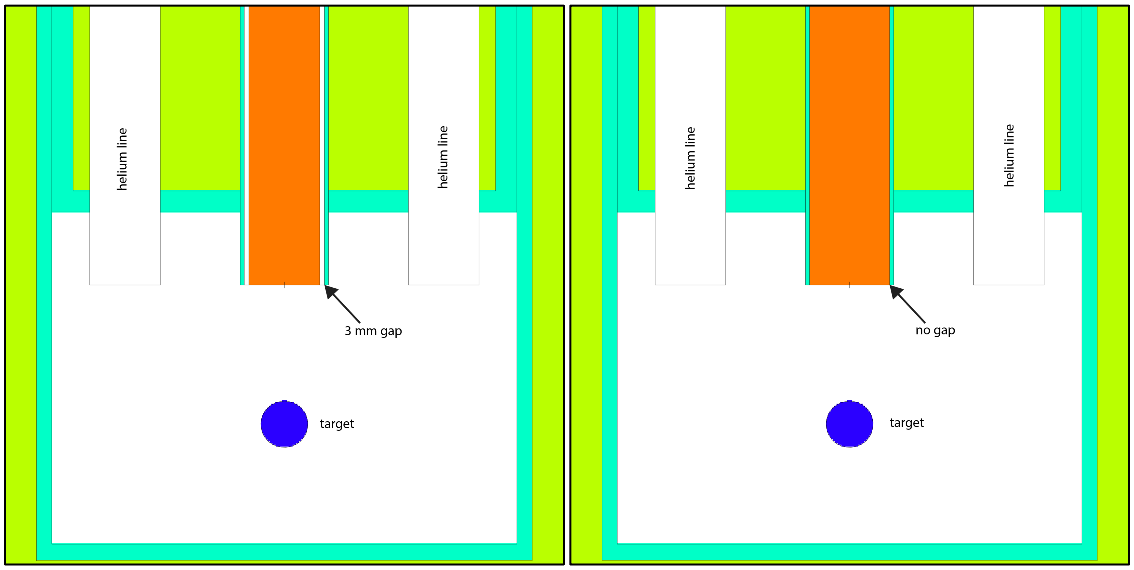

Figure 7: Close up view of the target retrieval mechanism near the target location. Left panel depicts the geometry with 3 mm gap. The geometry without a gap is shown in the right panel.

The resulting dose rate fields obtained with a geometry that does not include a gap between the target retrieval rod and the surrounding shielding in the vertical shaft is shown in Figure 8. One can see a dramatic reduction of streaming radiation along the target retrieval rod (these maps to be compared with the results in Figure 6). For reference, the resulting dose rates on top of the target retrieval mechanism (same location as depicted in Figure 5) is less than 0.1 mrem/hr for both neutrons and photons.

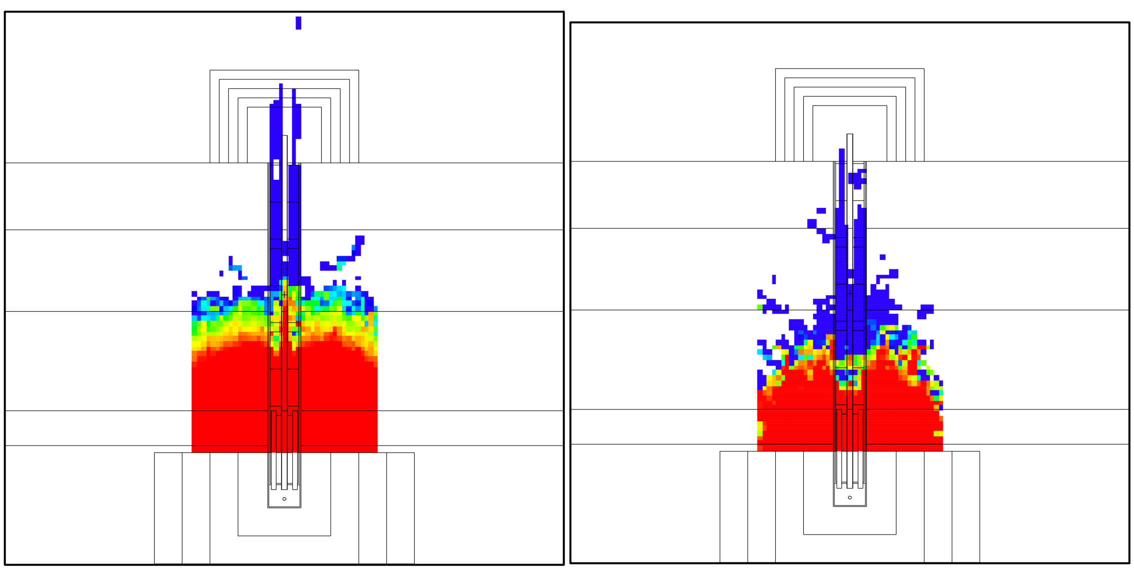

Figure 8: Dose rate fields calculated in the geometry with no gap between the target retrieval rod and the surrounding shielding. Left panel depicts the results for neutron and right panel shows the dose rate field map for photons. Red color depicts dose rates of 1 rem/hr and higher and blue shows dose rate fields of 1 mrem/hr or lower.

Conclusions and future work

We have setup and run multiple MCNPX models exploring the shielding issues in the vertical target insert/retrieval mechanism shaft of the Mo-99 production facility. We calculated the reference dose rates on top of the target retrieval mechanism for multiple scenarios and identified areas for more in-depth studies required.

The dose rates for the reference (minimum shielding) scenario are about 500 rem/hr for neutrons and 150 rem/hr for photons on top. By introducing one dogleg in the helium cooling lines and two shielding plugs (steel and borated polyethylene 30 cm each) we can reduce the dose rates on top down to about 2 rem/hr. The 3-mm gap between the target retrieval rod and the shielding insert creates a radiation-streaming path that prevents further reduction in dose rates on top. In our study we used 304.8 cm of regular concrete separating the service alley and the lower level containing the accelerator farm. The presented mesh tally results of dose rate fields indicate a possibility of reducing this concrete layer by 70-100 cm (the top layer is 73 cm thick). Reduction of the concrete thickness has a potential to lower the cost of the production facility. The details (amount) of this reduction will depend strongly on the optimized shielding design of the target insert/retrieval mechanism port.

We have shown that even relatively small gap between the target retrieval rod and the surrounding shielding results in significant dose rate consequences in the service alley. Clearly more effort is needed to carry out a detailed optimization study of the vertical target retrieval mechanism port that will be conducted in close collaboration with the engineering team. Next iteration of the shielding optimization will look at the design of the target retrieval mechanism and study the tolerances as dictated by the engineering requirements. This next study will be able to conclude the reduction of the concrete layer thickness separating the accelerator level from the service alley.